Articles

Molecular Determinants of the Anticonvulsant Felbamate Binding Site in the *N*-Methyl-D-Aspartate Receptor

Huai-Ren Chang[†] and Chung-Chin Kuo*[,†,‡]

Department of Physiology, National Taiwan University College of Medicine, 1, Jen-Ai Road, First Section, Taipei 100, Taiwan, and Department of Neurology, National Taiwan University Hospital, 7, Chung San South Road, Taipei 100, Taiwan

Received June 8, 2007

The antiepileptic effect of felbamate (FBM) is ascribable to gating modification of NMDA receptors. Using site-directed mutagenesis and electrophysiological studies, we found that single-point mutations of four pairs of homologous residues in the external vestibule of the receptor pore, namely V644(NR1)-L643(NR2B) (the two inner pairs) and T648(NR1)-T647(NR2B) (the two outer pairs), significantly decrease FBM binding. Moreover, double mutations involving either the inner or the outer pair always show cooperative (nonadditive) effects on FBM binding, whereas double mutations involving both inner and outer pairs always show additive (noncooperative) effects. Most interestingly, triple mutations of any three of the four critical residues essentially abolish the effect of FBM. These findings indicate that T648(NR1)/T647(NR2B) and V644(NR1)/L643(NR2B) act cooperatively to contribute directly to the "outer binding region" and "inner binding region" in the FBM binding site, respectively. The outer and inner binding regions, however, seem to contribute independently to FBM binding. We conclude that residues L643 and T647 in NR2B as well as homologous residues V644 and T648 in NR1 are the major, and very likely the exclusive, molecular determinants constituting the FBM binding site in the NMDA receptor.

Introduction

Felbamate (FBM; 2-phenyl-1,3-propanediol dicarbamate)[a] is a potent new-generation anticonvulsant for different types of seizures that are refractory to other anticonvulsants in both children and adults.[1–3] Although it has been reported that FBM may inhibit voltage-gated Na^+ channels[4,5] and potentiate γ-aminobutyric acid type A receptors,[6–8] the major antiepileptic effect of FBM at therapeutic concentrations seems to be at least partly ascribable to inhibition of the *N*-methyl-D-aspartate (NMDA) receptor.[7,9–11] FBM is shown to selectively bind to NMDA channels which are at the open and especially desensitized states rather than at the closed state.[12,13] Such selectivity of FBM binding to the open/desensitized channels well explains the use-dependent inhibition of NMDA currents and consequently the nonsedative anticonvulsant effect of FBM. Also, FBM accelerates the activation kinetics of the NMDA channel and slows the recovery from channel desensitization.[13] Moreover, FBM modifies NMDA channel gating via a one-to-one binding stoichiometry (one FBM per NMDA receptor) and has quantitatively the same enhancement effect on NMDA and glycine binding to the NMDA receptor.[12] The gating-modification activities of FBM are similar to those of ifenprodil (a phenylethanolamine) which also has an activity-dependent inhibitory effect on NMDA currents.[14,15] Although structurally different, both FBM and ifenprodil seem to favor the conformational changes induced by NMDA on the NMDA receptor, namely activation and desensitization.

It has been shown that the high-affinity binding site of ifenprodil is located in the amino terminal domain of NR2B.[14,16] However, the location and molecular determinants of the FBM binding site in the NMDA receptor remain largely unknown. According to the general consensus on the topology of ionotropic glutamate receptors (NMDA and non-NMDA receptors), each NMDA receptor subunit has three transmembrane segments (M1, M3, and M4), a reentrant loop (M2), an extracellular N-terminus (the amino terminal domain or ATD), and an intracellular C-terminus (Figure 1A; for a review see ref 17). Because FBM is an effective gating modifier, its binding site is very likely located in or near the regions related to gating. More recently, we found that FBM may act as an "opportunistic" pore blocker modulated by extracellular proton, suggesting that the FBM binding site is located at the junction of a widened and a narrow part of the ion conduction pathway of the NMDA receptor.[18] The preM1 and the C-terminal part of M3 (M3c) presumably constitute the main part of the external vestibule of the NMDA receptor pore[19,20] and are closely related to channel gating.[21–24] Moreover, the ATD and the preM1 have been shown to play a critical role in receptor desensitization.[25–27] In this study, we demonstrate that four residues in homologous positions of M3c of NR2B (L643 and T647) and NR1 (V644 and T648) subunits are critical for FBM binding to the NMDA receptor. Mutations of any three of the four residues would essentially abolish FBM action on the receptor. These residues may therefore constitute the major, and very likely the exclusive, binding ligands in the FBM binding site in NMDA receptors

* To whom correspondence should be addressed. Tel: (886)-2-23123456 ext 8236. Fax: (886)-2-23964350. E-mail: chungchinkuo@ntu.edu.tw.

[†] National Taiwan University College of Medicine.

[‡] National Taiwan University Hospital.

[a] Abbreviations: NMDA, *N*-Methyl-D-aspartate; FBM, felbamate; K_d, dissociation constant; K_{app}, apparent affinity; n_H, Hill coefficient.

10.1021/jm0706618 CCC: $40.75
Published on Web 02/27/2008

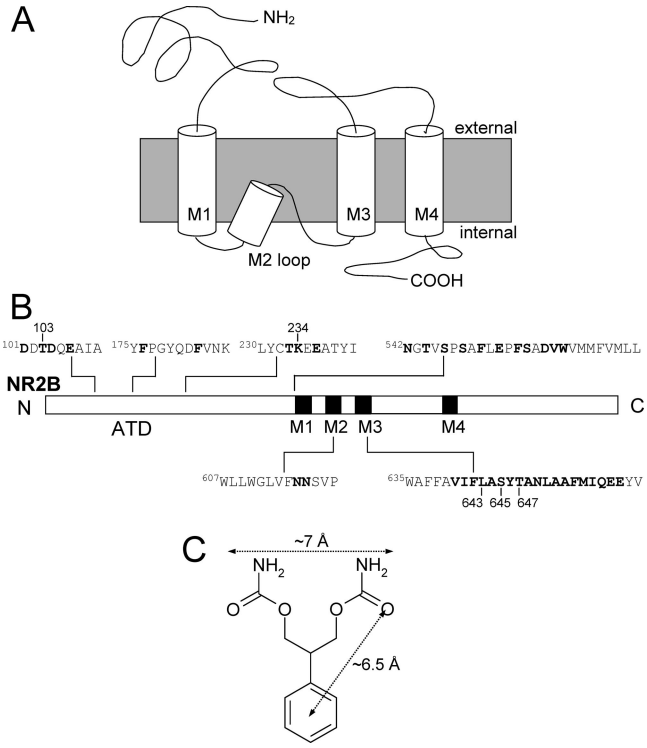

Figure 1. Topology and amino acid sequences of the NR2B subunit of the NMDA receptor and the chemical formula of the anticonvulsant FBM. (A) Topology of the NR2B subunit contains three transmembrane segments (M1, M3, and M4), a reentrant loop (M2), and a large extracellular amino terminal domain (ATD). (B) Amino acid sequences of the NR2B subunit. Alanine was substituted individually for each position (marked by boldface) in and around ATD, preM1, M2, and M3. The numbers indicate the position of a residue in the NR2B subunit. (C) Chemical structure of FBM.

and also mark the points of essential gating conformational changes of the channel.

Experimental Section

Molecular Biology and Expression of NMDA Receptors. The rat cDNA clones of NMDA receptors used in this study are the NR1a variant and the NR2B clone. The sequences of amino acid residues in the NR1 and NR2B subunits are numbered from the initiator methionine as in the original papers of NR1 and NR2B, respectively.[28,29] Site-directed mutagenesis was carried out using the QuikChange kit (Stratagene, La Jolla, CA). To prepare double mutations in the same subunit, cDNA templates that already contained one mutation were used for a second mutation. Mutations were verified by DNA sequencing, and two independent clones for each mutant were examined to ensure the lack of any inadvertent mutations. The full-length capped cRNA transcripts were then synthesized from each of NR1 and NR2B using T7 and T3 polymerases, respectively (mMESSAGE mMACHINE transcription kit, Ambion, Austin, TX). cRNA was stored in aliquots at −80 °C. To avoid the probability of formation of homomeric NR1 receptors, a mixture of NR1 and NR2 cRNAs in a ratio of 1:5 (i.e., 0.1–4 ng of NR1 and 0.5–20 ng of NR2; see also ref 23) was injected into *Xenopus* oocytes (stages V−VI). Oocytes were then maintained in the culture medium (96 mM NaCl, 2 mM KCl, 1.8 mM $MgCl_2$, 1.8 mM $CaCl_2$, 5 mM HEPES, and 50 μg/mL gentamycin, pH 7.6) at 18 °C for 2–3 days before electrophysiological studies. The culture medium was replaced daily.

Electrophysiological Recordings. Oocytes were placed in a small working-volume (<20 μL) perfusion chamber (OPC-1, AutoMate Scientific, Inc., San Francisco, CA) that is optimized for fast solution exchange. The NMDA currents were recorded at room temperature (~25 °C) with two-electrode voltage clamp (OC-725C amplifier; Warner Instrument, Hamden, CT). The microelectrodes, pulled from borosilicate capillaries and filled with 1 M KCl, had resistances of 0.5 to 4 MΩ. Oocytes were voltage-clamped at a membrane potential of −70 mV and continuously perfused with Mg^{2+}-free ND 96 solution (96 mM NaCl, 2 mM KCl, 0.3 mM $BaCl_2$, and 5 mM HEPES, pH 7.6). $CaCl_2$ was replaced by $BaCl_2$ here to minimize Ca^{2+}-activated Cl^- currents. FBM (Tocris Cookson, Inc., Bristol, UK) was dissolved in dimethyl sulfoxide to make a 100 mM stock solution. NMDA and glycine (Sigma, St. Louis, MO) were dissolved in water to make 100 mM and 10 mM stock solutions, respectively. The stock solutions were then diluted into Mg^{2+}-free ND 96 solution to make 0.01–1 mM FBM, 0.1 μM−1 mM NMDA, and 3 nM−30 μM glycine. The final concentration of dimethyl sulfoxide (1% or less) was found to have no detectable effect on NMDA currents. The highest FBM concentration used in this study was 3 mM, which is roughly its maximal solubility in water, and was made by dissolving FBM directly into Mg^{2+}-free ND 96 solution right before the experiment. To study the apparent affinity (i.e., refs 9 and 10; see also ref 16) of FBM, the concentration–response curves were fitted with the Hill equation

$$I = I_{max}/(1 + ([FBM]/K_{app})^{n_H}) \quad (1)$$

where I is the NMDA current in the presence of FBM, I_{max} is the maximum NMDA current, [FBM] is the FBM concentration, K_{app} is the apparent affinity of FBM binding to the receptor, and n_H is the Hill coefficient. K_{app} thus would be equal to the IC_{50} when the n_H is 1. For mutations displaying mean relative currents >60% at the highest FBM concentration tested (3 mM), the K_{app} values of FBM could only be rough estimates and are likely to be underestimated (see the Results).

Data Analysis and Homology Modeling for the Pore Region of NMDA Receptors. Data were acquired using the Digidata-1322A analog/digital interface with pCLAMP software (Axon Instruments, Foster City, CA). The sampling rates were 0.5–1 kHz, and all statistics are given as mean ± SEM. For comparisons between experimental groups, the Student's t test was used, and $p < 0.01$ was considered to be statistically significant. We also constructed a homology model of the NMDA receptor pore based on the sequence alignment of the alternating NR1 (S553-R659) or NR2B (F550-E658) subunit and the subunit of the MthK (1LNQ) potassium channel.[30] An NR1−NR1−NR2−NR2 orientation of subunits was assumed around the pore.[31] The sequences were aligned on the M2 loop and the M3 segment and then submitted to http://swissmodel.expasy.org/.

Results

Alanine Mutagenesis Scan Shows Two Critical Regions in the NR2B Subunit for FBM Inhibition on NMDA Currents. It has been shown that FBM has a stronger (~10-fold) effect on NMDA receptors containing NR2B than those containing NR2A or NR2C subunits.[9,10] We thus made a series of point mutations in and around ATD, preM1, M2, and M3c of the NR2B subunit (Figure 1B). For ATD, similar critical residues for the high-affinity binding site of ifenprodil were selected.[16] For M2, residues N615 and N616 were selected. These residues have also been shown to form the narrowest part of the NMDA receptor pore and binding sites for pore blockers such as Mg^{2+} and MK-801. For preM1 and M3c, most of the residues were selected because these two domains presumably constitute the wall of the external pore mouth. Given that FBM binding to the NMDA receptor may involve a variety of interactions (e.g., hydrophobic and hydrogen bonds; see the Discussion), we did not restrict our mutagenesis to specific residues chosen for their chemical properties but mutated each residue of the studied regions into alanine (i.e., alanine mutagenesis scan). If the selected residue is alanine itself, it is

Table 1. Effect of Point Mutations in the Amino Terminal, preM1, M2, and M3c Domains of NR2B on FBM Inhibition of the NMDA Currents[a]

mutation	mean relative current in 0.5 mM FBM (%)	*n*	mutation	mean relative current in 0.5 mM FBM (%)	*n*
wild type	68 ± 4	28	M2		
			N615A	66 ± 3	5
ATD			N616A	72 ± 2	5
D101A[b]	83 ± 4	4	M3c		
T103A[b]	85 ± 3	5	V640A	71 ± 4	5
D104A	75 ± 5	3	I641A[b]	84 ± 2	7
E106A	74 ± 3	3	F642A	75 ± 5	6
F176A[b]	84 ± 5	7	L643A[b]	90 ± 3	8
F182A	72 ± 3	3	A644C	73 ± 5	4
T233A[b]	84 ± 2	4	S645A[b]	85 ± 4	6
K234A[b]	85 ± 3	6	Y646A	74 ± 3	6
E236A[b]	83 ± 3	5	T647A[b]	89 ± 2	8
Pre-M1			A648C	73 ± 5	4
N542A	73 ± 4	5	N649A	NF	13
T544A	69 ± 3	5	L650A	76 ± 5	6
S546A	64 ± 2	3	A651T	72 ± 5	5
S548A	76 ± 5	4	A652T[b]	83 ± 3	6
F550A	62 ± 3	3	F653A	NF	11
E552A	77 ± 5	3	Post-M3		
F554A	NF	12	M654A	71 ± 6	3
S555A	72 ± 2	4	I 655A	76 ± 3	5
D557A	75 ± 3	4	Q656A	70 ± 5	4
V558A	71 ± 2	3	E657A	61 ± 3	3
W559A	NF	10	E658A	65 ± 5	4

[a] The mean relative current in 0.5 mM FBM is defined by the ratio between the amplitude of the sustained currents elicited by 100 μM NMDA (with 10 μM glycine) in 0.5 mM FBM-containing and FBM-free external solutions in the same oocyte and is expressed as mean ± SEM. [b] Mutations showing a significant ($p < 0.01$) decrease in FBM sensitivity. ATD, amino terminal domain; NF, nonfunctional; n, number of tested oocytes.

substituted into cysteine or threonine (e.g., A644C, A648C, A651T, and A652T). All mutants were screened by measuring the inhibition of NMDA currents by 0.5 mM FBM. The mutant receptors that have a significantly different ($p < 0.01$) response from the wild-type receptor are considered to contain mutations at the key positions. These key mutations roughly correspond to those mutants that showed a current decrease <16% in 0.5 mM FBM (vs 32% for the wild-type receptor; Table 1). Of the 41 mutations tested (all of which generated functional channels, except F554A, W559A, N649A, and F653A), we found 11 key positions (Table 1). Interestingly, these 11 key mutations are clustered in two regions, namely ATD and M3c, of the NR2B subunit. The concentration–response curves of FBM were then constructed for each of the 11 mutant and the wild-type receptors (Figure 2 and Table 2). The K_{app} value of FBM for the wild-type receptor (containing NR1/NR2B subunits) is 0.87 mM, quantitatively consistent with the previously reported values in recombinant NR1/NR2B receptors (e.g., 0.52–0.93 mM).[9,10] The 11 mutant receptors could be subdivided into two groups according to the degree of reduction of apparent FBM affinity. One group includes D101A, F176A, T233A, E236A, I641A, and A652T mutant receptors, whose K_{app} values (~2–3 mM) are ~2–3-fold higher than that of the wild-type receptor (Table 2). The other group includes T103A, K234A, L643A, S645A, and T647A mutant receptors, which have more pronounced effects on FBM sensitivity with K_{app} values >4 mM (Table 2; the K_{app} values can only be roughly estimated because even ~3 mM (a saturating concentration) FBM inhibits the NMDA current by no more than ~40%; see Figure 2B).

Different Mutations of T647 in M3c of the NR2B Subunit Could Significantly Change the Inhibitory Effect of FBM on NMDA Currents. We have identified several key residues (for FBM binding) clustered in two separated regions, namely ATD (e.g., T103 and K234) and M3c (e.g., L643, S645 and T647), of the NR2B subunit. To study the possible

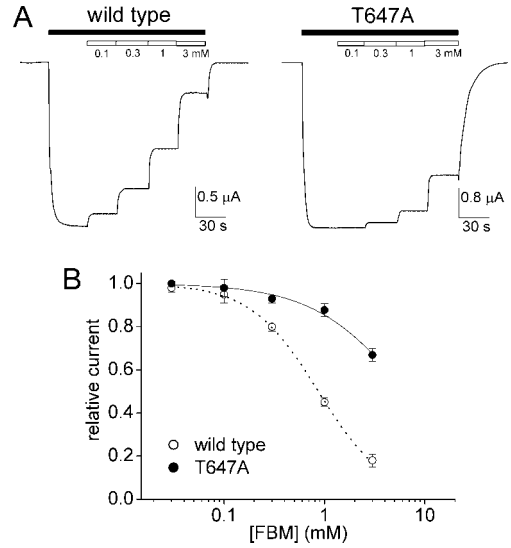

Figure 2. FBM concentration–response curves of the wild-type and T647A(NR2B) mutant receptors. (A) NMDA receptors obtained from oocytes coexpressing wild-type NR1 with either the wild-type or mutant NR2B subunits were elicited by application of 100 μM NMDA plus 10 μM glycine and then FBM at increasing concentrations (0.1−3 mM) was applied to the oocytes. The bars above the current traces indicate the application of the agonists (NMDA and glycine; black bar) and FBM (white bar). The current trace in T647A mutation (right panel) is typical of the other receptors containing key NR2B mutations (e.g., T103A, K234A, L643A, and S645A), which have much smaller responses to FBM than the wild-type receptor (left panel). (B) FBM concentration–response curves were obtained with the same experimental protocol as that described in part A. The relative current is defined by the ratio between the amplitude of the sustained currents elicited by 100 μM NMDA pulse in FBM-containing and FBM-free external solution in the same oocyte, and is expressed as mean ± SEM ($n = 36$ and 10 for the wild-type and T647A mutant receptors, respectively). The relative current is plotted against the FBM concentration, and the lines are the best fits to the mean values of the data using eq 1.

interactions between these key residues and FBM in more detail, we further examined the effects of other mutations of these key residues on the apparent FBM affinity. The key residues which have an K_{app} value >4 mM in alanine scanning (T103, K234, L643, S645, and T647) were then mutated to specific amino acids containing different side chains (e.g., charged group: R, K, and E; aromatic group: W and F). At L643, mutations into either a charged group (L643R, L643K, and L643E) or an aromatic group (L643W and L643F) have a more pronounced effect on the K_{app} of FBM than alanine substitution (~10–15-fold increase in the K_{app} value, Figure 3A). At T647, sensitivity to FBM is significantly reduced by single point mutations T647R, T647K, and T647E (~10–23-fold increase in the K_{app} value) but is increased by single mutations T647W and T647F (~3–11-fold decrease in the K_{app} value, Figure 3A). Different mutations of T647 thus could result in more than 200-fold changes in the K_{app} of FBM. T647W and T647F mutations do not alter the NMDA affinity (K_{app} of NMDA = 15.2 ± 0.4 and 14.6 ± 0.2 μM, respectively, $n = 5$–6, data not shown) but lead to much smaller NMDA currents than the wild-type receptor (i.e., <1 μA vs ~5 μA, $n = 5$–6). We suppose that the enhanced apparent affinity, or more precisely the enhanced inhibitory effect, of FBM on these mutants may be ascribed to the development or enhancement of pore-blocking effect of FBM when FBM binds to the pore region (which is already jeopardized by the much bulkier side chains of the mutant residues W and F) to exert the gating-modification effect. The

Table 2. K_{app} of FBM in NMDA Receptors Containing Single or Double Mutations at the Key NR2B Residues[a]

NR2B mutant	K_{app} (mM)	n_H	K_{app}(mutant)/ K_{app}(wild type)
wild type	0.87 ± 0.02	1.02 ± 0.03	
amino terminal domain			
D101A	2.76 ± 0.03	1.00 ± 0.02	3.2
T103A	4.21 ± 0.05	1.06 ± 0.03	4.8
F176A	2.77 ± 0.04	1.00 ± 0.01	3.2
T233A	2.56 ± 0.03	1.00 ± 0.02	2.9
K234A	4.31 ± 0.06	1.05 ± 0.04	4.9
E236A	2.18 ± 0.03	1.01 ± 0.02	2.5
M3c domain			
I 641A	2.45 ± 0.03	1.07 ± 0.05	2.8
L643A	5.64 ± 0.07	1.01 ± 0.01	6.5
S645A	4.23 ± 0.04	1.03 ± 0.02	4.9
T647A	6.50 ± 0.03	0.99 ± 0.02	7.5
A652T	2.92 ± 0.02	1.05 ± 0.04	3.3
double mutation			
L643A+T647A	34.5 ± 0.13	1.03 ± 0.02	40
L643C+T647A	18.6 ± 0.11	0.99 ± 0.02	21
L643A+T103A	5.07 ± 0.06	1.00 ± 0.01	5.8
L643A+K234A	6.33 ± 0.05	0.98 ± 0.03	7.3
L643A+S645A	6.68 ± 0.07	1.02 ± 0.02	7.7
T647A+T103A	6.73 ± 0.03	1.00 ± 0.02	7.7
T647A+K234A	7.00 ± 0.09	1.03 ± 0.03	8.0
T647A+S645A	7.04 ± 0.06	1.05 ± 0.04	8.1
S645A+T103A	6.28 ± 0.03	1.00 ± 0.02	7.2
S645A+K234A	7.10 ± 0.10	1.07 ± 0.05	8.2
S645A+ I641A	4.43 ± 0.04	1.04 ± 0.01	5.1
T103A+K234A	4.14 ± 0.05	1.01 ± 0.02	4.8

[a] The K_{app} and n_H values of FBM are obtained from concentration−response curves using the same experimental protocol described in Figure 2 and are expressed as mean ± SEM (n = 6–10 for each mutant receptor and n = 36 for the wild-type receptor). The K_{app}(mutant)/K_{app}(wild type) values are the estimates of relative changes in K_{app} and are the ratios between the mean K_{app} of the mutant and that of the wild type channels.

development of pore-blocking effect of FBM on T647W mutant receptor is also supported by the findings that although the mutation increases the apparent affinity of FBM, 0.3 mM FBM no longer enhances the small current elicited by low concentrations (e.g., 6 μM) of NMDA which significantly enhances the wild-type NMDA currents because of gating-modification effect (i.e., enhancement by 1 ± 0.5% vs 35 ± 3%, $p < 0.05$, $n = 5$, data not shown).[13] On the other hand, substitution of T647 with cysteine (T647C) or serine (T647S) produced smaller changes in the apparent affinity of FBM (K_{app} = 2.61 and 1.09 mM, respectively; Figure 3A) than the other T647 mutant receptors (see above). Thus, at T647, the presence of a hydroxyl group (found in T and S, which may serve as a hydrogen-bond donor) and the relative size of the side chain (T and C) are both important for FBM binding and its functional consequences (see the Discussion). These findings suggest that T647 and probably also L643 are directly involved in FBM binding. In contrast, a different profile is observed with mutations of the other key residues T103, K234 (in ATD), and S645 (in M3c). At these positions, different mutations (e.g., T-to-R, T-to-K, T-to-W, and T-to-F) give no significantly different or even less effect on the K_{app} of FBM from alanine substitution (Figure 3B). These residues thus do not seem to interact directly with FBM. Instead, mutations at these positions could allosterically interfere with FBM action through the effect on local structure or gating behavior of the NMDA receptor. For example, mutations at S645 may change the spatial orientation of L643 and T647, and then interfere with the inhibitory effect of FBM (see below).

Double Mutations at L643 and T647 of the NR2B Subunit Show Additive Effects on the Apparent Affinity of FBM. L643 and T647 presumably are adjacent residues on roughly the same face of an α-helix, the presumable secondary structure of M3c. To examine the possibility of direct contribution of L643 and T647 to the FBM binding site, we studied the effects of double mutations on the K_{app} of FBM (Figure 4). L643A+T647A double mutation indeed has a much greater effect than either single mutation (K_{app} increased by ~40-, ~6-, and ~7-fold for L643A+T647A, L643A, and T647A mutations, respectively; Figure 4A and Table 2). To further evaluate that two residues in double mutations interact independently or cooperatively for FBM binding, we used double mutant cycle analysis to calculate a coupling coefficient (Ω) and coupling energy ($\Delta\Delta G_{int}$) for each pair of mutations.[32] If the two residues are coupled in energy terms, there will be a coupling energy $\Delta\Delta G_{int}$ given by

$$\Delta\Delta G_{int} = \Delta\Delta G_{A12} - (\Delta\Delta G_{A1} + \Delta\Delta G_{A2}) = RT\ln(Kd_A Kd_{A12}/Kd_{A1}Kd_{A2}) \quad (2)$$

$$\Omega = Kd_A Kd_{A12}/Kd_{A1}Kd_{A2} \quad (3)$$

where Kd_A, Kd_{A1}, Kd_{A2}, and Kd_{A12} are the dissociation constant (Kd) of wild type (A), single mutants (A_1 and A_2), and double mutant (A_{12}) for FBM binding, respectively. R is the gas constant, and T is the absolute temperature. We have demonstrated that FBM binds to the NMDA receptor with a one-to-one binding stoichiometry based on different kinetic and steady-

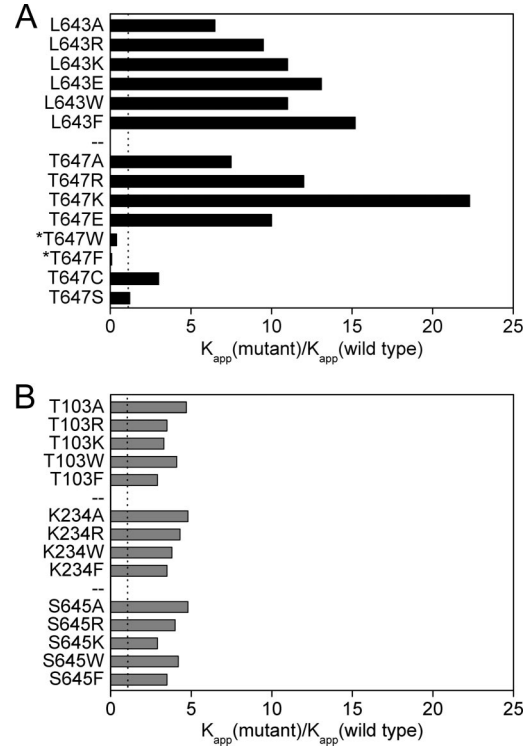

Figure 3. Summary of the effects of different mutations at the key NR2B residues on the apparent affinity of FBM. (A and B) A number of different mutations (e.g., mutated into R, K, E, W, and F) were studied at residues L643, T647 (part A), T103, K234, and S645 (part B) in the NR2B subunit. The same experimental protocol and analysis were done as in Figure 2 (n = 6–10 for each mutant receptor). The K_{app} values for each mutant receptor are obtained from the fits to the FBM concentration–response curves using eq 1 (n_H = 0.99–1.06) and are expressed relative to that of the wild-type receptor. The dotted line represents no change in the apparent affinity of FBM as compared to the wild-type receptor. The asterisks (*) indicate that the mutants enhance rather than decrease the apparent affinity of FBM.

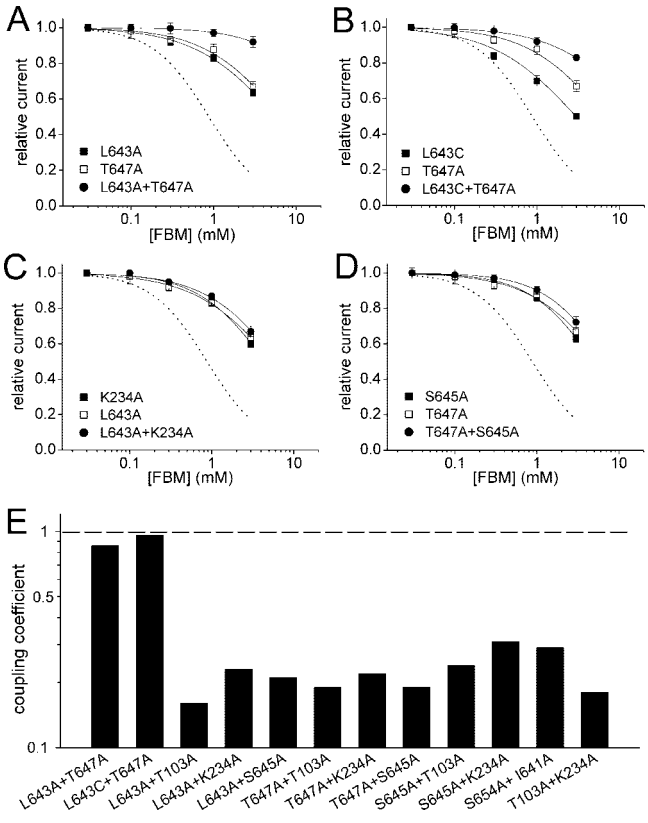

Figure 4. FBM concentration–response curves of the receptors with double mutations in NR2B. (A−D) FBM concentration–response curves in the wild-type and double mutant (L643A+T647A, L643C+T647A, L643A+K234A, and T647A+S645A) receptors were constructed using the same experimental protocol described in Figure 2 (n = 6–10 for each mutant receptor), and the K_{app} values are summarized in Table 2. For clarity, only the fitting curves but not the data points of the wild-type receptor are shown (dotted lines). (e) The coupling coefficients (Ω) for double mutations are calculated using double-mutant cycle analysis (eq 3). Mutations of any two residues with independent (additive or noncooperative) effects would have a coupling coefficient of 1.0 (dashed line). Note that in this plot only L643A+T647A and L643C+T647A double mutations have coupling coefficients of ~1.

state data.[12,13] Also, the Hill coefficients (i.e., n_H values) in Table 2 are very close to ~1 for both the wild-type and most mutant receptors. These findings indicate that although the highest FBM concentration used in this study (~3 mM, which is roughly its maximal solubility in water) may not inhibit a large proportion of NMDA currents in some mutants, the K_{app} value fitted from the concentration–response curve should be the best (and also a reasonable) measure we can have for the affinity of FBM to the receptor. We thus took the K_{app} value of FBM as a first approximation of the K_d value in eqs 2 and 3. The reduction in the apparent FBM affinity of the double mutation L643A+T647A is consistent with an additive (noncooperative) effect (coupling coefficient = 0.83, Figure 4E). We further examined the effects of other double mutations at L643 and T647 on FBM sensitivity and found that effect of L643C+T647A double mutation is also additive (K_{app} increased by ~21-, ~3-, and ~7-fold for L643C+T647A, L643C, and T647A mutations, respectively; Figure 4B and a coupling coefficient of 0.96; Figure 4E). The additive feature strongly suggests that residues L643 and T647 independently contribute to the FBM binding site. If each of the single mutations decreases the apparent affinity of FBM because of an indirect effect on channel gating, then double mutations of both residues would not be independent but share a common pathway to affect FBM binding. In other words, even if the mutations separately contribute to redistribute the receptor to the states where FBM binding is more (or less) favorable, from then on the effects would coalesce to affect FBM binding via the same process of gating conformational changes, and consequently, the effects of double mutations would not be additive. FBM thus very likely interacts directly rather than allosterically (via the channel gating process) with residues L643 and T647. On the other hand, additive effects cannot be observed with the double mutations other than L643+T647. The double mutations combining L643A and any one of T103A, K234A, or S645A (these latter three single mutations also have significant effects on the K_{app} of FBM) show no additive effects on the K_{app} of FBM (Figure 4C and Table 2). The same findings are also obtained with the double mutations combining T647A and any one of T103A, K234A, or S645A (Figure 4D and Table 2). Moreover, the effects of double mutations S645A+T103A, S645A+K234A, S645A+I641A, and T103A+K234A on FBM sensitivity are not significantly greater than those of individual single mutations (Table 2). The coupling coefficients thus are significantly smaller than 1 (i.e., ~0.2–0.3) in these double mutations (Figure 4E). These findings would support the foregoing idea that these residues (e.g., T103 and K234 in ATD, and S645 in M3c) allosterically rather than directly contribute to FBM binding.

Residue T647 (but not L643) of the NR2B Subunit Plays a Pivotal Role Coupling FBM Binding and Channel Gating. We have shown that FBM is an effective gating modifier of the NMDA channel and has a ~2- to 4-fold higher affinity to the open and especially the desensitized channels than to the closed channels.[13] It would be interesting to see whether mutations of the foregoing residues that are directly or allosterically involved in FBM binding may also affect NMDA channel gating (e.g., alteration of the NMDA affinity to the NMDA receptor). Figure 5A shows NMDA concentration–response curves of the wild-type and selected NR2B mutant receptors. None of the mutants of the key residues significantly decrease the NMDA affinity to the receptor, and most of the mutant receptors (e.g., L643A, T103A, and K234A) have K_{app} values (~12–16 μM) of NMDA similar to that of the wild-type receptor (K_{app} = 14.4 μM). The reduced FBM sensitivity in these mutants (especially L643A and T647A) thus cannot be ascribed to any decrease in the NMDA affinity to the receptor, consistent with the foregoing idea that L643 and T647 directly rather than allosterically contribute to the FBM binding site. In contrast, it is interesting that T647A (K_{app} = 4.5 μM) and S645A (K_{app} = 7.6 μM) mutant receptors significantly enhance (~2–3-fold) the apparent affinity of NMDA to the receptor (i.e., shift concentration–response curves to the left), suggesting that T647 and S645 are also closely involved in the NMDA-dependent gating process of the receptor. Because T647A mutation enhances apparent NMDA affinity to the receptor, it would tend to redistribute the receptor to the states where NMDA binding is more preferable. Because FBM has a higher affinity toward the gating conformations induced by NMDA binding (i.e., the open and desensitized states of the channel), the effect of T647A on channel gating then should increase rather than decrease the apparent affinity of FBM. The experimental findings of "decreased" apparent affinity of FBM in T647A mutation (Figure 2 and Table 2) thus cannot be ascribed to an indirect (or allosteric) effect derived from channel gating. Moreover, the double (e.g., L643A+T647A(NR2B)) mutations which produced much more pronounced effects on the apparent FBM affinity (Figure 4A) did not cause more changes in NMDA affinity than that in single mutant T647A

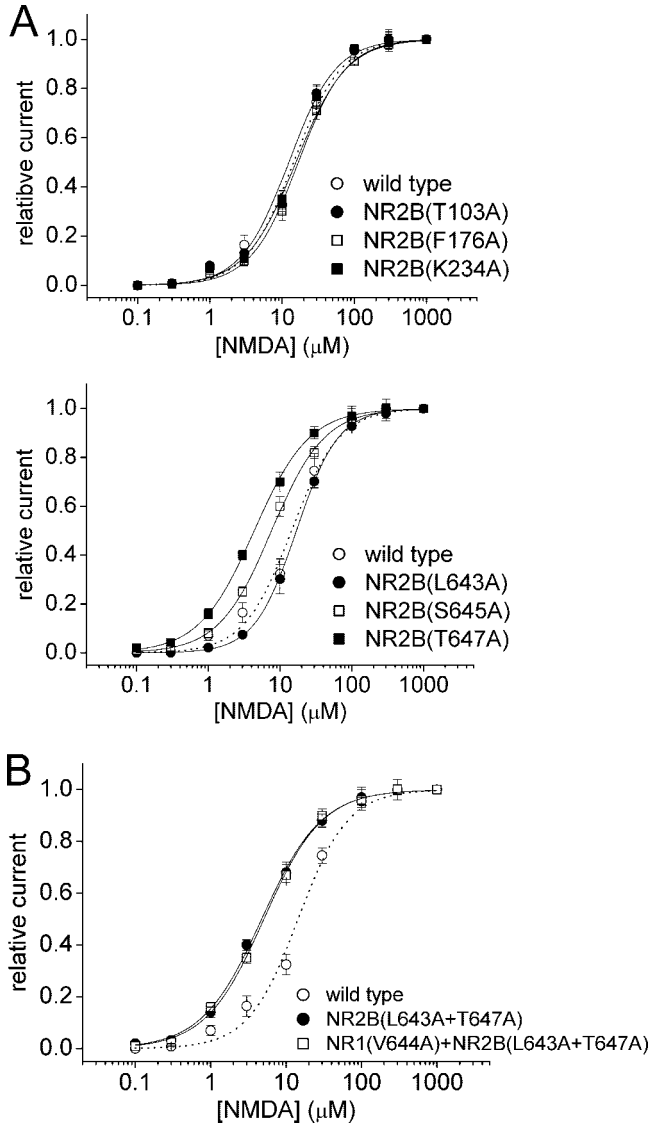

Figure 5. NMDA concentration–response curves of the wild-type and selected NR2B mutant receptors. (A) NMDA currents were elicited by application of 10 μM (saturating) glycine and different concentrations (0.1 μM to 1 mM) of NMDA at the wild-type and NR2B mutant receptors. The relative current is defined as the ratio between the sustained current amplitude in different concentrations of NMDA and that in 1 mM NMDA (approximating the I_{max}) and is plotted against the NMDA concentration. The lines are the best fits to the mean values of the data using the Hill equation ($I = I_{max}/(1 + (K_{app}/[NMDA])^{n_H})$, where I is the NMDA current in a given concentration of NMDA, I_{max} is the maximum current, [NMDA] is the NMDA concentration, K_{app} is the apparent affinity of NMDA to the NMDA receptor, and n_H is the Hill coefficient). The K_{app} values of NMDA are 14.4, 12.4, 16.7, 15.5, 16.8, 7.6, and 4.5 μM for the wild-type, T103A, F176A, K234A, L643A, S645A, and T647A mutant receptors, respectively. The n_H values are 1.3, 1.3, 1.3, 1.2, 1.5, 1.2, and 1.1 for the wild-type, T103A, F176A, K234A, L643A, S645A, and T647A mutant receptors, respectively (n = 8–14 for each different receptor). (B) The same experimental protocol and analysis were done as that in part A. The K_{app} values are 4.7 and 5.1 μM for double-mutant NR2B(L643A+T647A) and triple-mutant NR1(V644A)+NR2B(L643A+T647A) receptors, respectively. The n_H values are 1.3 and 1.2 for the double- and triple-mutant receptors, respectively (n = 5–6 for each mutant receptor).

(K_{app} of NMDA = 4.7–5.1 v.s. 4.5 μM, n = 5–6; Figure 5B). This finding also strongly argues against that T647 and L643 necessarily affect FBM binding because of their primary effect on channel gating. Along with the foregoing findings that T647

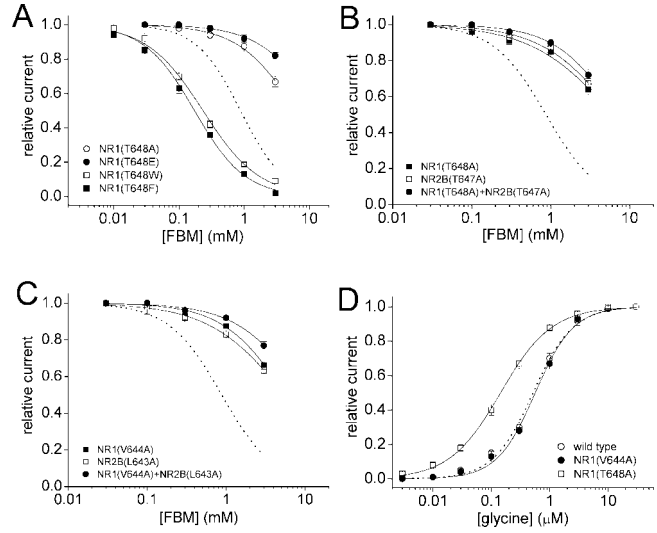

Figure 6. FBM and glycine concentration–response curves in NR1 single mutant or NR1+NR2B double mutant receptors. (A) The same experimental protocol and analysis were done as in Figure 2 (n = 6–8 for each different receptor). The K_{app} values are 5.78, 14, 0.23, and 0.17 mM for T648A, T648E, T648W, and T648F (NR1) single-mutant receptors, respectively. For clarity, only the fitting curve but not the data points of the wild-type receptor is shown (dotted line) in parts A−C. (B) The K_{app} values are 5.78, 6.50, and 7.09 mM for T648A(NR1), T647A(NR2B), and T648A(NR1)+T647A(NR2B) mutant receptors, respectively. (C) The K_{app} values are 5.76, 5.64, and 9.63 mM for V644A(NR1), L643A(NR2B), and V644A(NR1)+L643A(NR2B) mutant receptors, respectively. (D) Glycine concentration–response curves were constructed in the presence of 100 μM (saturating) NMDA with the same experimental protocol and analysis as that in Figure 5. The K_{app} values of glycine are 0.52, 0.56, and 0.14 μM for the wild-type, V644A(NR1), and T648A(NR1) mutant receptors, respectively. The n_H values are 1.3, 1.3, and 1.2 for the wild-type, V644A(NR1), and T648A(NR1) mutant receptors, respectively (n = 6–8 for each different receptor).

may directly contribute to the FBM binding site (Figures 3 and 4), it is very likely that T647 plays a pivotal role coupling FBM binding and channel gating (see the Discussion). On the other hand, S645 probably acts as a transducer relaying the gating effect of NMDA binding to the FBM binding site, and S645 mutations may well affect the local conformations of the adjacent T647 and L643. S645A mutation thus also mildly shifts the NMDA concentration–response curve (Figure 5A), but no additive effect is observed in L643A+S645A or T647A+S645A double mutations (Figure 4E).

Two Residues V644 and T648 in M3c of the NR1 Subunit Also Contribute to the FBM Binding Site. NMDA receptors are heterotetrameric channels composed of the NR1 and NR2 subunits, both contributing to the constitution of the pore region.[19,23,33] To determine whether the NR1 subunit also contributes to the FBM binding site, we further examined the K_{app} of FBM in NR1 mutant receptors (i.e., mutations of V644 and T648 in NR1, residues homologous to L643 and T647 in NR2B, respectively). Very much analogous to T647 mutations in NR2B, T648 mutations in NR1 also significantly decrease or increase the inhibitory effect of FBM on NMDA currents (Figure 6A). The effect of FBM is reduced by single-point mutations T648A and T648E (NR1) (~6.5- and ~16-fold increase in the K_{app} value, respectively), but is increased by single mutations T648W and T648F (NR1) (~4- and ~5-fold decrease in the K_{app} value, respectively). These results strongly suggest that residue T648(NR1) also contributes to FBM binding in a very similar way to that of T647(NR2B). Moreover, the

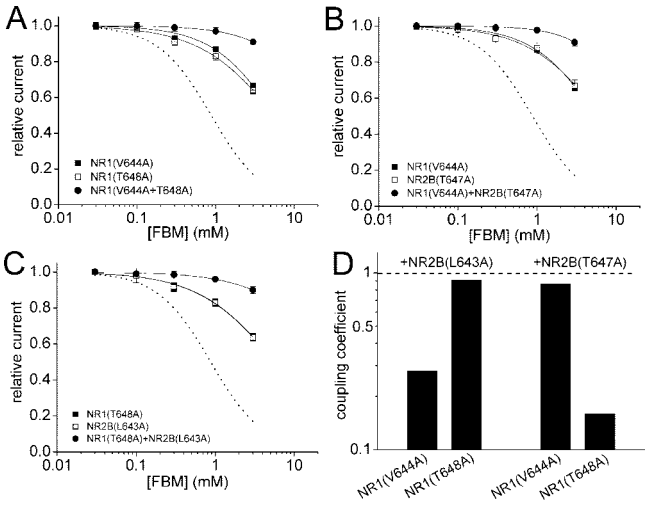

Figure 7. FBM sensitivity in double-mutant receptors with mutations of two nonhomologous critical residues in NR1 or NR2B. (A) FBM concentration–response curves in the wild-type and double-mutant receptors were constructed using the same experimental protocol described in Figure 2 (n = 6–8 for each mutant receptor). Analysis was done as in the previous figures. The K_{app} values are 5.76, 5.78, and 32.2 mM for V644A(NR1), T648A(NR1), and V644A+T648A(NR1) mutant receptors, respectively (n_H = 1.02–1.04). For clarity, only the fitting curve but not the data points of the wild-type receptor is shown (dotted lines) in parts A−C. (B) The K_{app} values are 5.76, 6.50, and 36.4 mM for V644A(NR1), T647A(NR2B), and V644A(NR1)+T647A (NR2B) mutant receptors, respectively (n_H = 0.98–1.03). (C) The K_{app} values are 5.78, 5.64, and 34.1 mM for T648A(NR1), L643A(NR2B), and T648A(NR1)+L643A(NR2B) mutant receptors, respectively (n_H = 1.01–1.06). (D) The coupling coefficients (Ω) for pairs of NR1 and NR2B mutations are calculated using double mutant cycle analysis (eq 3). The dashed line indicates a coupling coefficient of 1.0.

NR1 mutant receptor V644A has a ~6-fold increase in the K_{app} of FBM (Figure 6C), quantitatively similar to that of NR2B mutant receptor L643A. On the other hand, we also found in the NR1 mutations that T648A but not V644A enhances the glycine affinity to the receptor (K_{app} of glycine = 0.52, 0.14, and 0.56 μM for the wild-type, T648A, and V644A mutant receptors, respectively, n = 6–8; Figure 6D), a case very similar to the enhanced NMDA affinity in the corresponding NR2B mutant receptors.

The Four Pairs of Homologous Residues in Two NR1-NR2B Heterodimers Exclusively Make the FBM Binding Site. We have demonstrated that four residues in M3c of the NR2B (L643 and T647) and NR1 (V644 and T648) subunits are critically involved in FBM binding to the NMDA receptor. To determine individual contribution of the four critical residues to the FBM binding site, we further examined the effects of double mutations of these residues on the K_{app} of FBM. Figure 7 shows that double mutations of any two nonhomologous critical residues in NR1 and NR2B (e.g., V644A+T648A (NR1),V644A(NR1)+T647A(NR2B),L643A(NR2B)+T648A(NR1), and also L643A+T647A(NR2B) in Figure 4E) lead to additive (noncooperative) effects on the apparent affinity of FBM (coupling coefficients = 0.84–0.92; Figures 4E and 7D). However, in double mutations of two homologous residues such as V644A(NR1)+L643A(NR2B) and T648A(NR1)+T647A(NR2B), the additivity is much weaker (coupling coefficients = 0.28 and 0.16, respectively; Figure 7D). The significant negative coupling energy ($\Delta\Delta G_{int}$ = −0.8 and −1.1 kcal/mol, respectively, calculated by eq 2) further indicates that there is an attractive interaction between these two homologous residues in NR1 and NR2B. These findings strongly suggest that T648(NR1) and T647(NR2B) contribute similarly (or even equally) and act cooperatively to make the "outer binding region" in the FBM binding site, whereas V644(NR1) and L643(NR2B) contribute similarly and act cooperatively to make the "inner binding region" in the same binding site. The outer and inner binding regions, on the other hand, seem to contribute independently (noncooperatively) to FBM binding. Most interestingly, combination of any three point mutations of the four critical residues (L643 and T647 in NR2B; V644 and T648 in NR1) essentially abolishes the inhibitory effect of 3 mM FBM (a saturating concentration of FBM) on NMDA currents (Figure 8), but does not cause more changes in NMDA affinity than T647A single mutation (Figure 5B). These findings altogether indicate that the four pairs of homologous residues, namely V644(NR1)-L643(NR2B) and T648(NR1)-T647(NR2B), in two NR1-NR2B heterodimers directly and exclusively make the FBM binding site (see the Discussion).

Discussion

Residues V644(NR1)-L643(NR2B) and T648(NR1)-T647-(NR2B) Directly Contribute to the FBM Binding Site. We have shown that L643 and T647 in M3c of NR2B and their homologous residues (V644 and T648) in NR1 are critically involved in FBM binding to the NMDA receptor. Different mutations of T647(NR2B) and T648(NR1) significantly decrease or increase the inhibitory effect of FBM on NMDA currents and could result in more than 200-fold changes in the K_{app} of FBM (Figures 3A and 6A). Mutations of L643(NR2B) and V644(NR1) also significantly increase the K_{app} of FBM by ~6–15 times (Figures 3A and 6C). In this regard, it is interesting that T647A mutation also enhances the NMDA affinity to the receptor (Figure 5A). The effect of T647A on channel gating thus, if anything, should increase the apparent affinity of FBM rather than decrease it because FBM has a higher affinity to the open/desensitized than the closed channels.[13] Also, L643A mutation has no effect on channel gating or NMDA affinity (Figure 5A) but still significantly decreases the apparent affinity of FBM (Figure 3A and Table 2). Residues L643 and T647 thus very likely serve as a direct contributor to the FBM binding site rather than affect FBM affinity indirectly via a primary effect on channel gating. Moreover, double mutations in the same subunit, such as L643A+T647A(NR2B), L643C+T647A(NR2B), or V644A+T648A(NR1) lead to additive (noncooperative) effects on the apparent affinity of FBM (coupling coefficient = ~1; Figures 4A,B,E and 7A). The additivity strongly suggests that the two residues in the same subunit (L643-T647 in NR2B or V644-T648 in NR1) independently contribute to FBM binding. It is thus unlikely that the mutations of these residues are coupled to the channel gating process to affect FBM binding. Consistently, double mutations (e.g., NR2B(L643A+T647A)) produce much more pronounced effects on the apparent affinity of FBM (Figure 4A), and triple mutations (e.g., NR1(V644A)+NR2B(L643A+T647A)) essentially abolish the FBM effect on the receptor (Figure 8), but they do not cause more changes in NMDA affinity than that in single mutation T647A (Figure 5B). Also, it is unusual to completely wipe out the effect of a gating modifier by mutations of the ligands which are just allosterically related to the drug binding site (especially when channel gating itself is only so trivially affected by the mutations). We therefore conclude that the FBM binding site is directly and exclusively constituted by the four pairs of homologous residues, namely V644(NR1)-L643(NR2B) (the two inner pairs) and T648(NR1)-

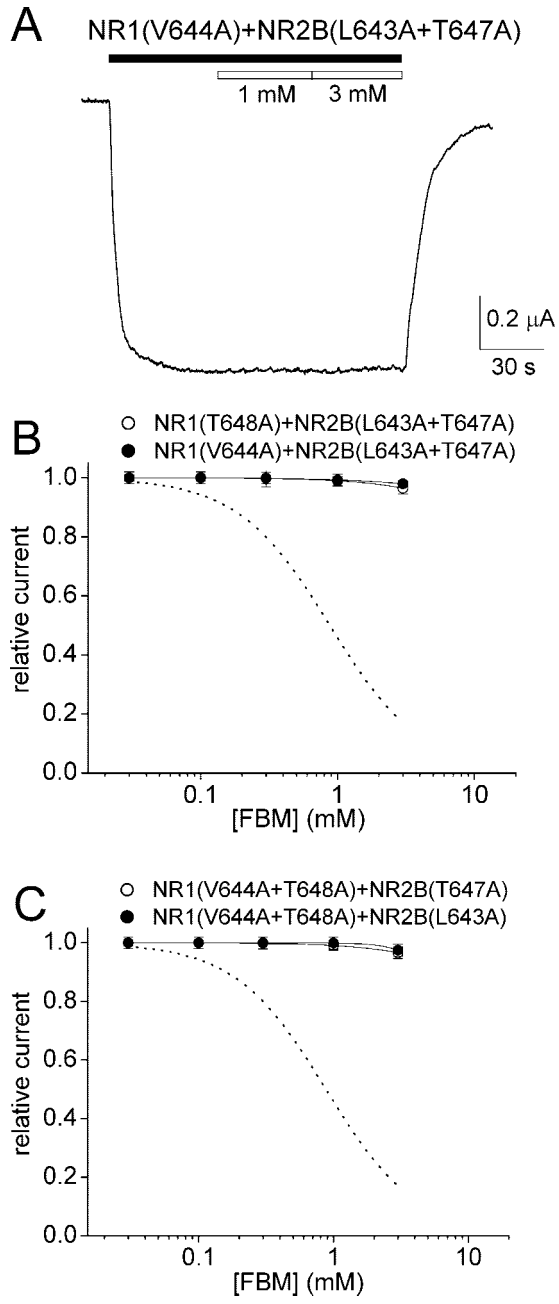

Figure 8. Lack of inhibitory effect of FBM on NR1+NR2B triple mutant receptors. (A) The experimental protocols were the same as those in Figures 2–4. Even the highest concentration (3 mM) of FBM has little inhibitory effect on NMDA currents of NR1-(V644A)+NR2B(L643A+T647A) triple mutant receptor. (B and C) FBM concentration–response curves in the wild-type and triple mutant receptors (NR1(T648A)+NR2B(L643A+T647A), NR1-(V644A)+NR2B(L643A+T647A) in part B; NR1(V644A+T648A)+NR2B(T647A), NR1(V644A+T648A)+NR2B(L643A) in part C) were constructed as in Figure 2 ($n = 6$ for each mutant receptor). For clarity, only the fitting curves but not the data points of the wild-type receptor are shown (dotted line).

T647(NR2B) (the two outer pairs), in two NR1-NR2B heterodimers (see below).

The FBM Binding Site Is Located at the External Pore Mouth of the NMDA Receptor. The internal vestibule of the NMDA channel is probably formed by M2 loops from two NR1 and two NR2 subunits,[33] whereas the external vestibule is formed by residues on preM1, M3c, and the N-terminal part of M4 ($M4_N$).[19,20] For more detailed topology of the external vestibule, M3c probably is responsible for the deeper part leading to the narrow constriction (presumable "selectivity filter") in the pore, whereas preM1 and $M4_N$ may form more superficial parts.[20] Residues L643, T647 (NR2B), V644, and T648 (NR1), which exclusively make the FBM binding site, are located in the middle part of M3 in sequence (Figure 9A) and are thus very likely located in the external vestibule of the channel pore. Although no atomic structural resolution of the NMDA receptor is available at present, there is a general consensus that the pore region of the NMDA receptor shares evolutionary and structural kinship with K^+ channels and their relatives.[33–37] We therefore constructed a homology model of the pore region of NMDA receptors for the open state (Figure 9C), which was derived from the crystal structure of the MthK K^+ channel.[30] It is interesting that similar to the inner helix of an inverted K^+ channel, M3 of NMDA receptors may well represent a major pore-lining domain. In addition, M3 is α-helical, with the tip of M2 loop (defined by the Q/R/N site which is N616 in NR1 or N615 in NR2B) positioned about halfway across it.[19] The two residues of the same subunit critically involved in FBM binding (i.e., L643 and T647 of NR2B, or V644 and T648 of NR1) thus face the same side (Figure 9B), consistent with the finding that both residues in the same subunit are also solvent accessible to methanethiosulfonate (MTS) reagents.[19,20] In other words, they very likely line the lumen of the channel pore. In contrast, residue S645(NR2B) is close to L643 and T647 but does not face the same side as L643 and T647, consistent with its solvent inaccessibility to MTS reagents. Moreover, residues N615, L643, and T647 in NR2B as well as homologous residues in NR1 (i.e., N616, V644, and T648) probably form the bottom part of the external vestibule (Figure 9C). In this regard, it is interesting to note that the pore-blocking effect of FBM on the NMDA channel is not evident at pH 7.4 but becomes manifest at pH 8.4,[18] reminiscent of the Na^+-dependent "opportunistic" pore blocking effect of diclofenac on the Na^+ channel pore.[38] Moreover, the inhibitory effect of FBM on NMDA currents is antagonized by external but not internal Na^+.[18] FBM thus also is an "opportunistic" pore blocker of the NMDA channel, very likely with its binding site located at the junction of a relatively widened and a narrow part of the external vestibule of the channel pore. This picture is consistent with the presumable structural features of L643-T647 depicted by Figure 9C.

The FBM Binding Site Is Composed of Two Binding Regions Made by Symmetrically Arranged M3c Domains of the NR1 and NR2B Subunits. There is always significant cooperative effect on FBM binding in double mutations of the homologous critical residues (i.e., residues from the same pairs). For example, the coupling coefficients are 0.28 and 0.16 for T648A(NR1)+T647A(NR2B) and V644A(NR1)+L643A(NR2B), respectively (Figure 7D). The cooperative feature strongly suggests that homologous residues T648(NR1) and T647(NR2B) (in the outer pairs) interact with each other to make the "outer binding region", whereas V644(NR1) and L643(NR2B) (in the inner pairs) also interact with each other to form the "inner binding region" of the FBM binding site. The cooperative interactions between these homologous residues would furthermore indicate that T648(NR1)-T647(NR2B) or V644(NR1)-L643(NR2B) in the same NR1-NR2B heterodimer are located in close proximity to each other in spatial orientation (Figure 10 and see below). This finding is also well in line with the idea that the NR1-NR2 heterodimer is the functional unit in tetrameric NMDA receptors.[39] On the other hand, the additive effect on FBM

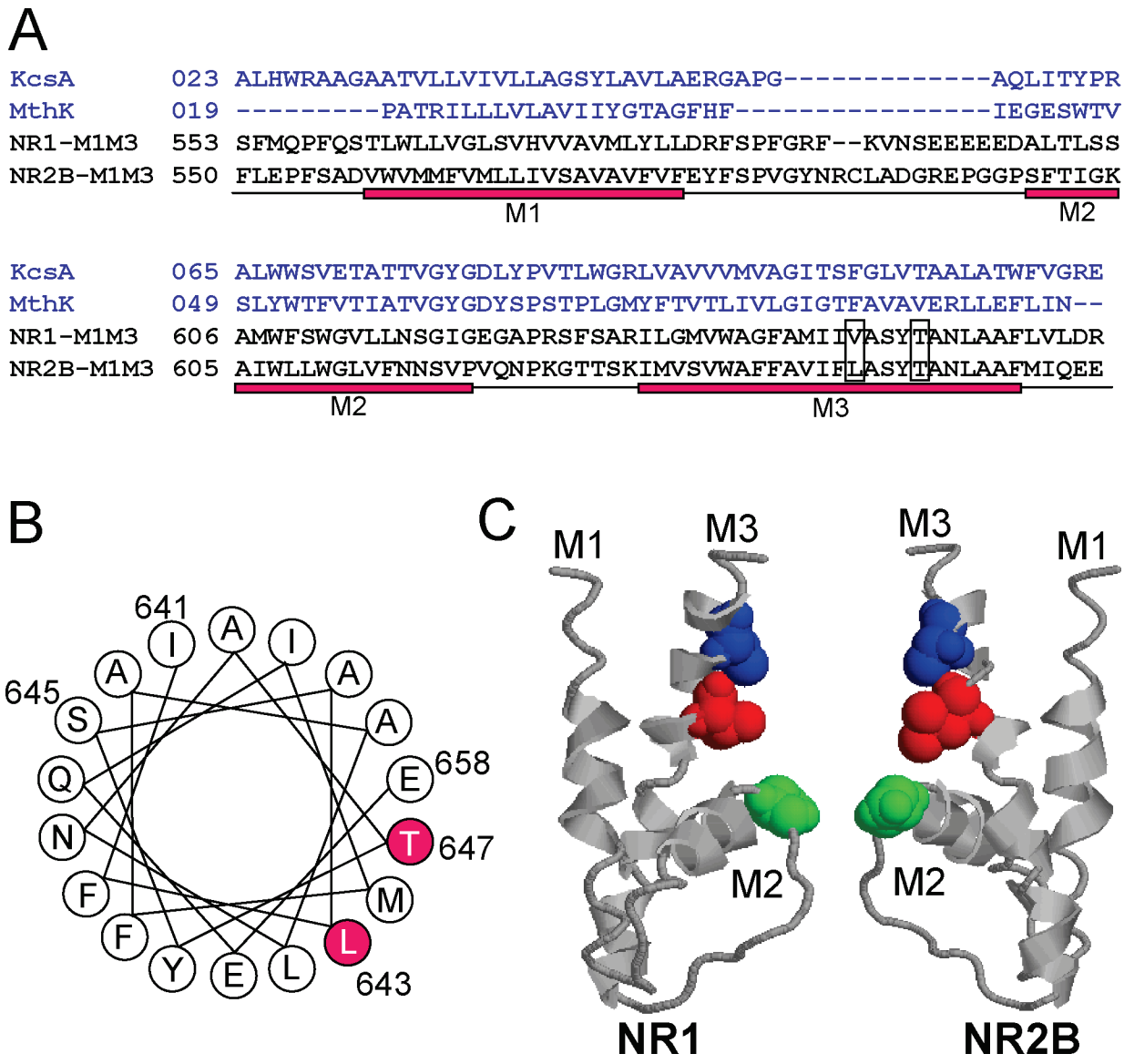

Figure 9. Homology modeling for the pore region of NMDA receptors based on the crystal structure of the MthK potassium channel. (A) Sequence alignment of the alternating NR1 (residues S553-R659) or NR2B (residues F550-E658) subunit and the subunits of the KcsA and the MthK potassium channels. (B) Helical wheel plot for 18 residues (I641-E658) within M3 of the NR2B subunit. The number denotes the position of a residue in the NR2B subunit. Two critical residues for FBM binding, namely L643 and T647, are shown as red symbols with white labels. (C) A homology model for the pore region of NMDA receptors is based on the crystal structure of the MthK (open conformation) potassium channel. The M1, M2, and M3 segments from two opposite NR1-NR2B subunits are shown as cartoons, with the front and back subunits removed for clarity. The asparagine residue at the Q/R/N site of NR2B (i.e., N615 which is located at the tip of M2 loop) as well as L643 and T647 (and homologous residues of NR1, i.e., N616, V644, and T648) are shown as spacefills and are colored green, red, and blue, respectively. These residues probably form the deeper part of the external vestibule of the NMDA channel pore.

binding in double mutations of any two critical residues from different pairs (with coupling coefficients of ~1; Figure 7D) indicates that the inner (i.e., V644(NR1)-L643(NR2B)) and outer (i.e., T648(NR1)-T647(NR2B)) binding regions of the binding site contribute independently to FBM binding, despite their close proximity to each other (vertical distance ~6 Å in an α-helix). The FBM binding site thus seems to have a fairly symmetrical build-up along the axis of the NMDA channel pore at least in M3c (but see ref 40). Based on our experimental data and homology modeling of the pore region, we propose a stereographic model describing the FBM binding site consisting of two independent (outer and inner) binding regions with two pairs of symmetrically arranged and mutually interacting binding residues in each region (Figure 10). The two homologous hydrophilic threonine residues (i.e., T648(NR1)-T647(NR2B)) in each NR1-NR2B heterodimer probably interact with each other to put two hydroxyl groups in a favorable spatial orientation and therefore interact with the two opposite carbamate groups of one FBM molecule with hydrogen bonds. On the other hand, the two homologous hydrophobic residues (i.e., V644(NR1)-L643(NR2B)) in each NR1-NR2B heterodimer may interact to form the hydrophobic binding site for the phenyl group of FBM.

Residue T647(NR2B) Plays a Pivotal Role in FBM Binding, Ion Permeation, NMDA-Dependent Channel Gating, and Extracellular pH-Sensitive Conformational Changes. In all glutamate receptors, the M3c domain contains a highly conserved nine amino acid sequence (the "SYTANLAAF" motif). Substitutions of residues in this motif of the NMDA

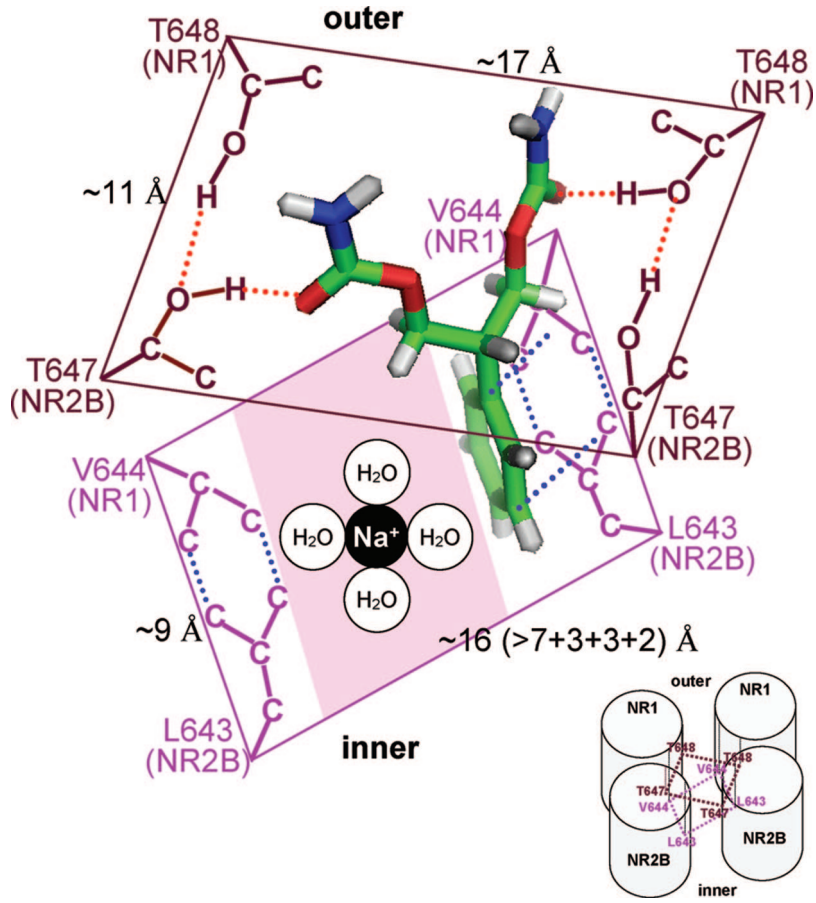

Figure 10. Stereographic model of the FBM binding site. The FBM binding site in the NMDA receptor is composed of two independent (inner and outer) binding regions with four relatively symmetrically arranged and cooperatively interacting residues in each region. FBM has a phenyl group and a symmetrical propanediol dicarbamate group (Figure 1C). Two critical residues (for FBM binding) in the same subunit, namely V644 and T648 in NR1 or L643 and T647 in NR2B, should be ~6 Å apart on roughly the same face of a presumable α-helix of M3c (Figure 9B). The outer binding region of the FBM binding site thus is formed by the four homologous residues of two T648 in NR1 and two T647 in NR2B (the T648(NR1)-T647(NR2B) plane, colored brown), and the inner binding region is formed by the four homologous residues of two V644 in NR1 and two L643 in NR2B (the V644(NR1)-L643(NR2B) plane, colored pink). These are depicted with an NR1-NR1-NR2-NR2 orientation of subunits around the pore.[31] The outer T648(NR1)-T647(NR2B) plane is rotated by 40° relative the inner V644(NR1)-L643(NR2B) plane because of the α-helical structure of M3c (see also the inset figure, showing the positions of the binding ligands on the M3c columns viewed from the exterolateral side). For clarity, only side chains of these critical residues are shown. Red and blue dotted lines indicate the hydrogen-bond and the hydrophobic interactions, respectively. Threonine, which has a hydroxyl group, on either position 648(NR1) or 647(NR2B) may serve as a hydrogen-bond donor. Two homologous residues T648(NR1) and T647(NR2B) in the NR1-NR2B heterodimer interact with each other (probably with a hydrogen bond) to form each of the two parts of the outer binding region, which most likely binds to the oxygen or nitrogen atoms of the two carbamate groups of FBM (i.e., presumably also with a hydrogen bond). On the other hand, the hydrophobic side chains of V644(NR1) and L643(NR2B) in the NR1-NR2B heterodimer also interact with each other to establish two identical hydrophobic inner binding regions (presumable a six-carbon structure), and the phenyl group of FBM presumably would bind to one of the two regions. We have demonstrated that FBM binds to the NMDA receptor via a one-to-one binding process (one FBM per NMDA receptor). The 3D structure of FBM is constructed by the Dundee PRODRG Server (http://davapc1.bioch.dundee.ac.uk/programs/prodrg/), and is shown as sticks with green carbon, red oxygen, blue nitrogen, and gray hydrogen. The linear distance between the center of the phenyl group and the oxygen or nitrogen atom of the carbamate group is ~6.5 Å, and thus, the vertical height of FBM is well consistent with the distance between T647 and L643 in NR2B (or between T648 and V644 in NR1). The horizontal distance of the two oxygen or nitrogen atoms on the opposite carbamate groups is ~7 Å. If the T648(NR1)-T647(NR2B) plane has a roughly rectangular shape, the diagonal distance of the outer binding region is estimated to be ~20 Å with the usual bond lengths (between O−H···O, C−C, and so on) taken into consideration. The width and length of the plane at the outer binding region are thus estimated to be ~11 and ~17 Å, respectively. Each of the two carbamate groups of FBM would then well fit to bind to each "side" of the outer region with a hydrogen bond, respectively. When the phenyl group of FBM is bound to one of the two inner binding regions, the remaining space (pink area) of the pore at the V644(NR1)-L643(NR2B) plane should be at least ~7 Å in width for the passage of traveling hydrated ions (e.g., Na^+, because FBM is chiefly a gating modifier rather a pore blocker at physiological pH). Taking the C−C or C−O bond length (~1.5 Å) into consideration, we estimate the width and length of the "plane" at the inner binding regions as ~10 and ~16 Å, respectively.

receptor have been shown to significantly alter channel gating,[20–24] indicating that M3c plays an essential role in NMDA channel gating. In this study, we found that two NR2B single mutations (S645A and T647A) at this conserved motif show an enhancement effect on NMDA affinity to the receptor (Figure 5A). Interestingly, this mild but definite (~2–3-fold) enhancement of NMDA affinity in T647A(NR2B) mutation is quantitatively consistent with the previous report that FBM has a ~2–4-fold higher affinity to the open/desensitized than to the closed channels.[13] On the other hand, mutation of the other critical residue for FBM binding (i.e., L643 in NR2B), which is not in the conserved SYTANLAAF motif, does not alter NMDA affinity to the receptor. Recently, we have shown that FBM may act as an "opportunistic" pore blocker of the NMDA channel modulated by extracellular proton.[18] The FBM binding site (the binding ligands for

FBM) in the NMDA channel thus should be located in the pore region closely related to pH-sensitive gating conformational changes. Consistently, Low et al. reported that clustered residues in both the M3c domain (e.g., T648 in NR1 and T646 in NR2A, which correspond to T647 in NR2B) and the adjacent linker to the ligand-binding domain S2 (M3-S2 linker) of NR1 and NR2 are closely related to the proton-sensitive channel gating.[41] Residue T647(NR2B) and very likely also T648(NR1) thus may not only contribute directly to the FBM binding site, but also play a pivotal role orchestrating FBM binding, ion permeation, NMDA-dependent channel gating, and extracellular pH-sensitive conformational changes at the external vestibule of the channel pore.

Pharmaceutical Implications. NMDA receptor antagonists have been shown to have a broad-spectrum antiepileptic effect on experimental seizure models and thus have generated considerable interest. Unfortunately, in clinical trials, most NMDA receptor antagonists were found to have serious neurobehavioral complications which limited their further pharmaceutical development. FBM is so far the only approved anticonvulsant that evidently modulates NMDA receptor activity in therapeutic conditions. In this study, we characterize the FBM−NMDA receptor interactions in detail and forward a stereographic model depicting the key features of FBM binding. The proposed binding model not only explains the action of FBM but also suggests the functional moieties in the FBM molecule essential for its antiepileptic effect. Although FBM is a potent, nonsedative anticonvulsant, it has been limited to a second-line choice in most clinical conditions because of the risk of idiosyncratic hepatotoxicity and hematotoxicity.[1–3] Hopefully, the proposed molecular model of FBM action may serve as a rational basis for possible structural modifications of FBM, so that new anticonvulsants with less adverse reactions but unaffected (or even enhanced) therapeutic effect could be more efficiently developed.

Acknowledgment. We thank Drs. S. Nakanishi and K. Williams for sharing cDNAs encoding NR1a and NR2B subunits. This work was supported by Grant No. NSC 96-2320-B-002-009 from the National Science Council and Grant No. NHRI-EX96-9606NI from the National Health Research Institutes, Taiwan. H.-R. C. was a recipient of the M.D.-Ph.D. Predoctoral Fellowship from the National Health Research Institutes, Taiwan.

References

(1) Borowicz, K. K.; Piskorska, B.; Kimber-Trojnar, Z.; Malek, R.; Sobieszek, G.; Czuczwar, S. J. Is there any future for felbamate treatment? *Pol. J. Pharmacol.* **2004**, *56*, 289–294.

(2) Pellock, J. M.; Faught, E.; Leppik, I. E.; Shinnar, S.; Zupanc, M. L. Felbamate: Consensus of current clinical experience. *Epilepsy Res.* **2006**, *71*, 89–101.

(3) Rogawski, M. A.; Loscher, W. The neurobiology of antiepileptic drugs. *Nat. Rev. Neurosci.* **2004**, *5*, 553–564.

(4) Pisani, A.; Stefani, A.; Siniscalchi, A.; Mercuri, N. B.; Bernardi, G.; Calabresi, P. Electrophysiological actions of felbamate on rat striatal neurons. *Br. J. Pharmacol.* **1995**, *116*, 2053–2061.

(5) Taglialatela, M.; Ongini, E.; Brown, A. M.; Di Renzo, G.; Annunziato, L. Felbamate inhibits cloned voltage-dependent Na+ channels from human and rat brain. *Eur. J. Pharmacol.* **1996**, *316*, 373–377.

(6) Rho, J. M.; Donevan, S. D.; Rogawski, M. A. Barbiturate-like actions of the propanediol dicarbamates felbamate and meprobamate. *J. Pharmacol. Exp. Ther.* **1997**, *280*, 1383–1391.

(7) Rho, J. M.; Donevan, S. D.; Rogawski, M. A. Mechanism of action of the anticonvulsant felbamate: opposing effects on *N*-methyl-D-aspartate and gamma-aminobutyric acid A receptors. *Ann. Neurol.* **1994**, *35*, 229–234.

(8) Simeone, T. A.; Otto, J. F.; Wilcox, K. S.; White, H. S. Felbamate is a subunit selective modulator of recombinant gamma-aminobutyric acid type A receptors expressed in Xenopus oocytes. *Eur. J. Pharmacol.* **2006**, *552*, 31–35.

(9) Harty, T. P.; Rogawski, M. A. Felbamate block of recombinant N-methyl-D-aspartate receptors: selectivity for the NR2B subunit. *Epilepsy Res.* **2000**, *39*, 47–55.

(10) Kleckner, N. W.; Glazewski, J. C.; Chen, C. C.; Moscrip, T. D. Subtype-selective antagonism of *N*-methyl-D-aspartate receptors by felbamate: insights into the mechanism of action. *J. Pharmacol. Exp. Ther.* **1999**, *289*, 886–894.

(11) Subramaniam, S.; Rho, J. M.; Penix, L.; Donevan, S. D.; Fielding, R. P.; Rogawski, M. A. Felbamate block of the *N*-methyl-D-aspartate receptor. *J. Pharmacol. Exp. Ther.* **1995**, *273*, 878–886.

(12) Chang, H.-R.; Kuo, C.-C. Characterization of the gating conformational changes in the felbamate binding site in NMDA channels. *Biophys. J.* **2007**, *93*, 456–466.

(13) Kuo, C.-C.; Lin, B.-J.; Chang, H.-R.; Hsieh, C.-P. Use-dependent inhibition of the *N*-methyl-D-aspartate currents by felbamate: a gating modifier with selective binding to the desensitized channels. *Mol. Pharmacol.* **2004**, *65*, 370–380.

(14) Gallagher, M. J.; Huang, H.; Pritchett, D. B.; Lynch, D. R. Interactions between ifenprodil and the NR2B subunit of the *N*-methyl-D-aspartate receptor. *J. Biol. Chem.* **1996**, *271*, 9603–9611.

(15) Kew, J. N.; Trube, G.; Kemp, J. A. A novel mechanism of activity-dependent NMDA receptor antagonism describes the effect of ifenprodil in rat cultured cortical neurons. *J. Physiol.* **1996**, *497*, 761–772.

(16) Perin-Dureau, F.; Rachline, J.; Neyton, J.; Paoletti, P. Mapping the binding site of the neuroprotectant ifenprodil on NMDA receptors. *J. Neurosci.* **2002**, *22*, 5955–5965.

(17) Dingledine, R.; Borges, K.; Bowie, D.; Traynelis, S. F. The glutamate receptor ion channels. *Pharmacol. Rev.* **1999**, *51*, 7–61.

(18) Chang, H.-R.; Kuo, C.-C. Extracellular proton-modulated pore-blocking effect of the anticonvulsant felbamate on NMDA channels. *Biophys. J.* **2007**, *93*, 1981–1992.

(19) Beck, C.; Wollmuth, L. P.; Seeburg, P. H.; Sakmann, B.; Kuner, T. NMDAR channel segments forming the extracellular vestibule inferred from the accessibility of substituted cysteines. *Neuron* **1999**, *22*, 559–570.

(20) Sobolevsky, A. I.; Beck, C.; Wollmuth, L. P. Molecular rearrangements of the extracellular vestibule in NMDAR channels during gating. *Neuron* **2002**, *33*, 75–85.

(21) Jones, K. S.; VanDongen, H. M.; VanDongen, A. M. The NMDA receptor M3 segment is a conserved transduction element coupling ligand binding to channel opening. *J. Neurosci.* **2002**, *22*, 2044–2053.

(22) Kohda, K.; Wang, Y.; Yuzaki, M. Mutation of a glutamate receptor motif reveals its role in gating and delta2 receptor channel properties. *Nat. Neurosci.* **2000**, *3*, 315–322.

(23) Kashiwagi, K.; Masuko, T.; Nguyen, C. D.; Kuno, T.; Tanaka, I.; Igarashi, K.; Williams, K. Channel blockers acting at *N*-methyl-D-aspartate receptors: differential effects of mutations in the vestibule and ion channel pore. *Mol. Pharmacol.* **2002**, *61*, 533–545.

(24) Yuan, H.; Erreger, K.; Dravid, S. M.; Traynelis, S. F. Conserved structural and functional control of *N*-methyl-D-aspartate receptor gating by transmembrane domain M3. *J. Biol. Chem.* **2005**, *280*, 29708–29716.

(25) Krupp, J. J.; Vissel, B.; Heinemann, S. F.; Westbrook, G. L. N-terminal domains in the NR2 subunit control desensitization of NMDA receptors. *Neuron* **1998**, *20*, 317–327.

(26) Thomas, C. G.; Krupp, J. J.; Bagley, E. E.; Bauzon, R.; Heinemann, S. F.; Vissel, B.; Westbrook, G. L. Probing *N*-methyl-D-aspartate receptor desensitization with the substituted-cysteine accessibility method. *Mol. Pharmacol.* **2006**, *69*, 1296–1303.

(27) Villarroel, A.; Regalado, M. P.; Lerma, J. Glycine-independent NMDA receptor desensitization: localization of structural determinants. *Neuron* **1998**, *20*, 329–339.

(28) Moriyoshi, K.; Masu, M.; Ishii, T.; Shigemoto, R.; Mizuno, N.; Nakanishi, S. Molecular cloning and characterization of the rat NMDA receptor. *Nature* **1991**, *354*, 31–37.

(29) Monyer, H.; Sprengel, R.; Schoepfer, R.; Herb, A.; Higuchi, M.; Lomeli, H.; Burnashev, N.; Sakmann, B.; Seeburg, P. H. Heteromeric NMDA receptors: molecular and functional distinction of subtypes. *Science* **1992**, *256*, 1217–1221.

(30) Jiang, Y.; Lee, A.; Chen, J.; Cadene, M.; Chait, B. T.; MacKinnon, R. Crystal structure and mechanism of a calcium-gated potassium channel. *Nature* **2002**, *417*, 515–522.

(31) Schorge, S.; Colquhoun, D. Studies of NMDA receptor function and stoichiometry with truncated and tandem subunits. *J. Neurosci.* **2003**, *23*, 1151–1158.

(32) Carter, P. J.; Winter, G.; Wilkinson, A. J.; Fersht, A. R. The use of double mutants to detect structural changes in the active site of the tyrosyl-tRNA synthetase (Bacillus stearothermophilus). *Cell* **1984**, *38*, 835–840.

(33) Kuner, T.; Wollmuth, L. P.; Karlin, A.; Seeburg, P. H.; Sakmann, B. Structure of the NMDA receptor channel M2 segment inferred from the accessibility of substituted cysteines. *Neuron* **1996**, *17*, 343–352.

(34) Chen, G. Q.; Cui, C.; Mayer, M. L.; Gouaux, E. Functional characterization of a potassium-selective prokaryotic glutamate receptor. *Nature* **1999**, *402*, 817–821.

(35) Kuner, T.; Seeburg, P. H.; Guy, H. R. A common architecture for K+ channels and ionotropic glutamate receptors. *Trends. Neurosci.* **2003**, *26*, 27–32.

(36) Mayer, M. L.; Armstrong, N. Structure and function of glutamate receptor ion channels. *Annu. Rev. Physiol.* **2004**, *66*, 161–181.

(37) Panchenko, V. A.; Glasser, C. R.; Mayer, M. L. Structural similarities between glutamate receptor channels and K+ channels examined by scanning mutagenesis. *J. Gen. Physiol.* **2001**, *117*, 345–360.

(38) Yang, Y.-C.; Kuo, C.-C. An inactivation stabilizer of the Na^+ channel acts as an opportunistic pore blocker modulated by external Na^+. *J. Gen. Physiol.* **2005**, *125*, 465–481.

(39) Furukawa, H.; Singh, S. K.; Mancusso, R.; Gouaux, E. Subunit arrangement and function in NMDA receptors. *Nature* **2005**, *438*, 185–192.

(40) Sobolevsky, A. I.; Rooney, L.; Wollmuth, L. P. Staggering of subunits in NMDAR channels. *Biophys. J.* **2002**, *83*, 3304–3314.

(41) Low, C. M.; Lyuboslavsky, P.; French, A.; Le, P.; Wyatte, K.; Thiel, W. H.; Marchan, E. M.; Igarashi, K.; Kashiwagi, K.; Gernert, K.; Williams, K.; Traynelis, S. F.; Zheng, F. Molecular determinants of proton-sensitive *N*-methyl-D-aspartate receptor gating. *Mol. Pharmacol.* **2003**, *63*, 1212–1222.

JM0706618